Progress in Natural Science: Materials International xxx (xxxx) xxx–xxx

HOSTED BY

ELSEVIER

Contents lists available at ScienceDirect

Progress in Natural Science: Materials International

journal homepage: www.elsevier.com/locate/pnsmi

# $ZrO_2$-supported α-$MnO_2$: Improving low-temperature activity and stability for catalytic oxidation of methane☆

Jingbo Jia[a], Rui Ran[a,*], Ruiqi Guo[b], Xiaodong Wu[c], Duan Weng[a,c]

[a] Key Laboratory of Advanced Materials (MOE), School of Materials Science and Engineering, Tsinghua University, Beijing 100084, China
[b] School of Transportation Science and Engineering, Beihang University, Beijing 100083, China
[c] State Key Laboratory of New Ceramic and Fine Processing, School of Materials Science and Engineering, Tsinghua University, Beijing 100084, China

ARTICLE INFO

*Keywords:*
$MnO_2$
$ZrO_2$ support
Methane oxidation
Sulfur tolerance
Stability

ABSTRACT

The single phase α-$MnO_2$ and in-situ supported α-$MnO_2$/$ZrO_2$ with different ratios of Mn/Zr were synthesized by one-pot hydrothermal method. They showed superior activity for catalytic oxidation of methane and even better than that of 1% Pt/$Al_2O_3$. The $T_{50}$ of $MnO_2$/$ZrO_2$ catalysts with different ratios of Mn/Zr were located in the range of 315–335 °C at a WHSV of 90 L $g^{-1}$ $h^{-1}$, whereas that of Pt/$Al_2O_3$ was 380 °C. After sulfur ageing, the $MnO_2$/$ZrO_2$ catalysts with Mn/Zr ratio of 2:1 ($2MnO_2$/$1ZrO_2$) and 1:1 ($1MnO_2$/$1ZrO_2$) exhibited satisfying sulfur resistance in comparison to the pure $MnO_2$. The $2MnO_2$/$1ZrO_2$ catalyst also showed acceptable catalytic stability, and the addition of 10 vol% $CO_2$ had no obvious negative effect on its stability, whereas the addition of 2.6 vol% $H_2O$ caused slight but reversible decreasing methane oxidative activity.

## 1. Introduction

The natural gas has been considered as a desirable fuel due to its abundant, economical, relatively clean and safe. Compared with gasoline and diesel fuels, natural gas vehicles (NGVs) release ultralow polluting emissions, including $NO_x$, CO, $SO_2$ and fine particulates. However, a significant concern for NGVs is that the emission of unburned methane, which is recognized to contribute more to global warming than carbon dioxide. To meet the demands of much stricter environmental standards such as the Euro-VI standard for NGVs, abatement of unconverted methane in the exhaust become increasingly challenging. High-performance oxidative catalysts with high thermal stability and good low-sulfur tolerance are needed for this application.

Up to date, noble metal catalysts are widely used in oxidative catalysis. Due to the low cost and comparable catalytic oxidation activities, transition metal oxides have been considered as alternative catalysts to noble metal catalysts [1–4]. Among them, cobalt-based and chromium-based catalysts were extensively studied and exhibited excellent catalytic activity at low temperature [5–7]. However, due to the biotoxicity of cobalt and chromium, scientific researchers gradually looked forward to the environmental friendly transition metal oxides such as manganese-based catalysts.

Owing to the easily tunable structure and highly efficient redox properties of manganese oxides, especially $MnO_2$ was found to exhibit excellent catalytic performance in the oxidation of CO [8] and volatile organic compounds [9–11]. Lu et al. compared the catalytic oxidation activity of propane over different crystal phases $MnO_2$ and found that the catalytic performance decreased in the order of α- ≈ γ- > β- > δ-$MnO_2$. The α-$MnO_2$ exhibited the highest catalytic activity and its $T_{10}$ and $T_{90}$ were 204 °C and 290 °C, respectively [12]. Du et al. prepared 3D ordered mesoporous $MnO_2$ and its $T_{10}$ and $T_{90}$ for catalytic oxidation of toluene were 203 °C and 215 °C, respectively [13]. Niluka D. Wasalathanthri synthesized various meso-$MnO_x$ using an inverse surfactant micelle method and found that the meso-octahedral molecular sieves $MnO_2$ showed the highest conversion of methane among $MnO_x$ [14]. By now, $MnO_2$ has been considered as a potential catalyst to substitute precious metal catalysts for combustion of hydrocarbon. However, the obvious challenging problems for the manganese-based catalysts are their poor sulfur tolerance and thermal stability.

Zirconia has drawn a lot of attention as a catalyst support material due to its unique surface property [15]. Zhao et al. found that Mn/$ZrO_2$ was more stable during hydrothermal ageing than Mn/$TiO_2$ [16]. Qi and co-workers reported that the incorporation of $ZrO_2$ into $MnO_x$-$CeO_2$ mixed oxide increased the sulfur tolerance [17]. In this work, single phase α-$MnO_2$ with high catalytic activity is therefore attempted to be in-situ supported on $ZrO_2$ with different Mn/Zr ratios, in order to develop thermally stable and good sulfur resistant catalysts for the catalytic oxidation of methane.

☆ Peer review under responsibility of Chinese Materials Research Society.

* Corresponding author.
*E-mail address:* ranr@tsinghua.edu.cn (R. Ran).

https://doi.org/10.1016/j.pnsc.2018.04.005
Received 29 September 2017; Received in revised form 27 March 2018; Accepted 10 April 2018

## 2. Experimental

### 2.1. Catalyst preparation

The $ZrO_2$-supported $MnO_2$ ($MnO_2/ZrO_2$) samples was prepared by the one-step hydrothermal method. In a typical procedure, the Mn $(CH_3COO)_2$ solution was added drop wise into the mixed solution including $KMnO_4$, cetyltrimethyl ammonium bromide and $ZrO_2$ (BASF Chemical Company) with different ratios (Mn/Zr = 2, 1, 2/3) under continuous stirring. The slurry was then transferred into a Teflon lined stainless steel autoclave and kept at 140 °C for 2 h. After being cooled to room temperature, the solid was isolated by filtration, washed and dried at 85 °C. The resulting samples are named as $2MnO_2/1ZrO_2$, $1MnO_2/1ZrO_2$ and $2MnO_2/3ZrO_2$. For the pure α-$MnO_2$ samples, the process is similar to that of $MnO_2/ZrO_2$ except without the addition of $ZrO_2$.

The $Pt/Al_2O_3$ reference sample was synthesized by impregnation method according to a procedure reported in the previous literature [18]. The loading amount of Pt was 1 wt%.

### 2.2. Catalyst characterization

The phase composition of the samples was confirmed by X-ray diffraction (XRD) using an O8 discover (Siemens) instrument equipped with Cu $K_\alpha$ radiation at accelerating voltage and current of 40 kV and 40 mA, respectively. The morphology was observed with FE-SEM (S-5500, Hitachi) and HRTEM (Tecnai G2 F30 S-TWIN).

### 2.3. Catalytic activity test

The catalytic oxidation of methane was carried out using a fixed-bed reactor at a heating rate of 5 °C/min. In a typical test, the mixture of 200 mg fractionized (40–60 mesh) catalyst and 300 mg quartz sands were loaded in the reactor and the total flow rate through the reactor (1000 ppm $CH_4$, 10% $O_2$ balanced with $N_2$) was maintained at 300 mL/min. The effluent gas concentration was continuously monitored with an FT-IR gas analyzer (MKS MultiGas ™ 2030).

For the sulfur tolerance experiments, the catalysts were pretreated with a sulfur containing gas of under 22 ± 2 ppm $SO_2$ for 1 h at 250 °C. For the stability test, 400 mg catalyst and 600 mg quartz sands were employed for catalytic oxidation of methane at 400 °C. Other conditions are the same as the preceding activity test.

In order to evaluate the effect of $CO_2$ addition, 5 vol% and 10 vol% $CO_2$ was introduced via a mass flow controller. In the case of water vapor introduction, $H_2O$ was introduced by passing the feed $N_2$ stream through a water saturator at room temperature and 2.6% $H_2O$ was generated.

## 3. Results and discussion

### 3.1. Structure and morphology

The X-ray diffraction patterns of the catalysts are shown in Fig. 1. It can be seen that the diffraction peaks of the prepared $MnO_2$ occur at 12.8, 18.4, 25.8, 28.7, 37.5, 41.7, 49.3 and 59.8°, which agree well with tetragonal α-$MnO_2$ (JCPDS no. 44-0141). Broadening of the diffraction peaks suggests that as-synthesized α-$MnO_2$ is poor crystallized. The diffraction peaks of $ZrO_2$ can be identified at 30.2, 35.0, 50.4, 60.0 and 62.7°, which are ascribed to the diffractions of the (101), (110), (200), (211), and (202) crystalline planes of cubic phase $ZrO_2$ (JCPDS no. 49–1642), respectively. A series of different ratios of Mn/Zr oxides show the mixed phase of α-$MnO_2$ and $ZrO_2$ and no other phase are found. Decreasing the ratio of Mn/Zr within $MnO_2/ZrO_2$ samples, the peak of $MnO_2$ became much blunter than that of the pure $MnO_2$ due to the high dispersion of $MnO_2$ onto $ZrO_2$.

The morphologies of $MnO_2$ and $MnO_2/ZrO_2$ samples were investigated by SEM and TEM. As shown in Fig. 2 (A, B), the $MnO_2$ sample possesses the disorder nanofibers structure with the diameter of 5–20 nm and the length of 30–300 nm. The $ZrO_2$ exhibits irregular aggregates of nanoparticles and the porous surface (Fig. 2C). The growth of $MnO_2$ nanofibers on the $ZrO_2$ support are almost the same as the pure $MnO_2$, which indicates that $MnO_2$ exist on the surface of $ZrO_2$ but not incorporate into the lattice of $ZrO_2$. When the ratio of Mn/Zr was 2:1, the $ZrO_2$ becomes unclear in the vision of Fig. 2D and nearly completely submerged under the $MnO_2$ nanofibers. When the ratio of Mn/Zr decreased to 1:1, the resulting $MnO_2$ and $ZrO_2$ become intertwined and interconnected, as shown in Fig. 1E. For the $2MnO_2/3ZrO_2$ sample, the exposure of $MnO_2$ nanofibers are obviously sheltered by $ZrO_2$ aggregates (Fig. 1F). To further identify the microstructure of $MnO_2$ sample, the HRTEM image was obtained (the inset in Fig. 1B). The well-resolved lattice fringe distance is 0.31 nm, which corresponds to the (310) plane of α-$MnO_2$. After the addition of $ZrO_2$, the lattice fringe distance is not changed. Therefore, during the in-situ synthesis process of $MnO_2/ZrO_2$, the addition of $ZrO_2$ do not interrupt the growth and crystal structure of $MnO_2$, but only play the role of supports.

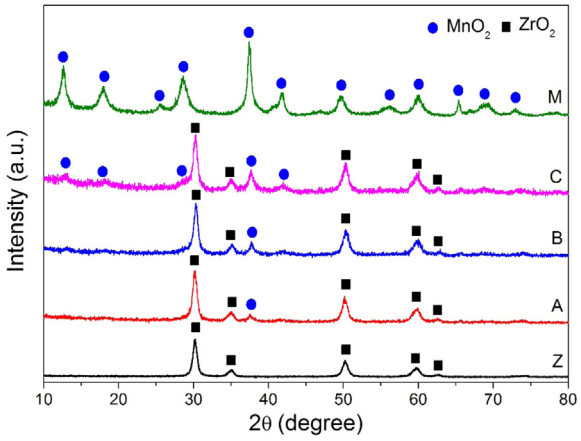


**Fig. 1.** XRD patterns of (M) $MnO_2$, (C) $2MnO_2/1ZrO_2$, (B) $1MnO_2/1ZrO_2$, (A) $2MnO_2/3ZrO_2$ and (Z) $ZrO_2$ samples. Symbols ■ and● represent the characteristic peaks of $ZrO_2$ and $MnO_2$.

### 3.2. Catalytic activity and sulfur tolerance

The catalytic activities of the as-prepared catalysts for methane oxidation are shown in Fig. 3. It can be seen that the $MnO_2$ and several $MnO_2/ZrO_2$ catalysts exhibit much higher activity for methane oxidation than 1% $Pt/Al_2O_3$. The $T_{50}$ and $T_{90}$ (the reaction temperature corresponding to methane conversions of 50% and 90%, respectively) of $MnO_2$ are 318 °C and 375 °C, while those of 1% $Pt/Al_2O_3$ are 380 °C and 495 °C, respectively. This indicates that $MnO_2$ has the potential to be an alternative low-temperature catalyst for methane oxidation. Compared to $MnO_2$, the pure $ZrO_2$ seems mostly inactive at in the temperature range of 200–450 °C so that it mainly plays the role of support during the catalytic oxidation of methane. The $T_{50}$ of the $MnO_2/ZrO_2$ catalysts are similar to that of $MnO_2$, while $T_{90}$ are 50–70 °C higher than that of $MnO_2$. No marked differences were observed between the $MnO_2/ZrO_2$ catalysts with different Mn/Zr ratios. Table 1 summarizes the overview of catalytic activity of metal oxides in recent literatures and it is hard to directly compare the activity due to the different conditions adopted in literatures. However, it can be seen that $MnO_2$ in this work is advantageous.

As a small amount of sulfur compound generally present in the commercial natural gas, the promising catalyst for methane oxidation needs to be resistant to sulfur poisoning. To investigate the influence of sulfur dioxide on the catalytic activity, the methane conversion of sulfur aged $MnO_2/ZrO_2$ samples ($MnO_2/ZrO_2$-S) were examined and the